Rippled state of double-layer quantum Hall systems

C. B. Hanna
Department of Physics, Boise State University, Boise, Idaho 83725
(Received 27 September 2001; published 31 October 2002)

The incommensurate phase of a bilayer quantum Hall state is found to have a ''rippled'' dipole charge density whenever the layers are unbalanced. This tunable dipole-density-wave instability could be detected by sensitive capacitance measurements and by anisotropic transport. We demonstrate this explicitly by carrying out a Hartree-Fock calculation of the layer densities and capacitance for a double-layer quantum Hall state at a total filling factor of 1.

DOI: 10.1103/PhysRevB.66.165325 PACS number(s): 73.43.Cd, 64.70.Rh, 71.10.Pm, 71.45.Gm

I. INTRODUCTION

The combination of reduced dimensionality and strong interparticle interactions can have spectacular effects on the nature of the ground-state and dynamical properties of many-particle systems. This is especially evident in the fractional quantum Hall regime,[1,2] where a strong magnetic field is applied perpendicular to a two-dimensional electron gas at very low temperatures. The powerful magnetic field quenches the kinetic energy of the electrons, so that interactions between electrons dominate the energetics. The result is a highly correlated, incompressible quantum-liquid ground state that supports fractionally charged excitations.[3] Even at integer filling factors (especially $\nu_T=1$), the combination of the quenched kinetic energy of interacting electrons plus extra electronic degrees of freedom (i.e., spin or multiple layers) can give rise to correlated ground states that support remarkable topological excitations, such as charged skyrmions.[4,5]

Another important class of systems in which reduced dimensionality and interactions strongly affect the ground state and dynamics are systems with charge-density-wave or spin-density-wave ground states,[6] and also systems that exhibit commensurate-incommensurate (CI) transitions.[7,8] Systems with charge- or spin-density-wave ground states occur most famously (although not exclusively) in quasi-one-dimensional materials, where the reduced dimensionality enhances fluctuation effects and leads to broken-symmetry ground states.[6] Systems exhibiting CI transitions have broken translational symmetry states with rich structures, most notably arrays of domain walls that arise from the competition between interparticle interactions and external periodic potentials.[7,8]

Double-layer quantum Hall (2LQH) systems can show both types of behavior: they support unusual fractionally charged topological excitations,[9,10] and they apparently exhibit a CI transition to a state with broken translational symmetry in the presence of a sufficently strong in-plane magnetic field.[9] It is interesting that in 2LQH systems, broken translational symmetry can coexist with the hidden off-diagonal long-range order[11] characteristic of quantum Hall states. The evidence for a CI transition in 2LQH systems is, however, indirect. Activation energy measurements show that a sufficiently large in-plane magnetic field drives a transition between two different types of many-body ground states,[12] and the strength of the in-plane magnetic field and the size of the energy gaps are consistent with the CI scenario.[9,12] In order to establish the nature of the competing quantum Hall ground states and the transition between them, additional types of experimental measurements are needed. Various types of experimental signatures of the CI scenario have been proposed, including predictions of the form of the energy gap,[13] a predicted Kosterlitz-Thouless transition,[10] anisotropic transport in narrow samples,[14] and the field dependence of the in-plane magnetization.[15,16] Here we propose that the CI transition in 2LQH systems could be studied directly by capacitance measurements, and by anisotropic transport produced by the dipole-density wave described below.

This paper examines a novel effect of unequal layer densities on the CI transition in 2LQH systems. (Interestingly, unequal layer densities can actually enhance the stability of the 2LQH state at total filling factor $\nu_T=1$.[17,18]) It is found that when the layer densities are not equal, they go from being uniform in the commensurate phase to becoming ''rippled'' in the incommensurate phase; this allows the CI transition to be detected by sensitive capacitance measurements.[17] The layer imbalance can be produced in two ways: most commonly by an external bias, but perhaps also spontaneously in a tilted sample with an unusually small capacitive charging energy and a sufficiently large interlayer tunneling.[19,20] We will focus here on bias-driven imbalance, since it is easier to achieve experimentally. In addition, capacitive techniques provide a quantitative measure of the interlayer exchange and pseudospin stiffness in 2LQH systems. This is illustrated in the following sections by a Hartree-Fock calculation of the layer densities and capacitances for a 2LQH state at a total filling factor $\nu_T=1$. Similar effects should, in principle, occur at other filling factors, although $\nu_T=1$ is probably most promising for experimental observation.

II. RIPPLED STATE

Interlayer Coulomb interactions at low filling factors can stabilize 2LQH states when the layer spacing is comparable to the separation between electrons within the layers.[21] Even at a total ''integer'' filling factor $\nu_T=1$, experiments indicate that the quantum-Hall ground states are stabilized by Coulomb interactions and do not require interlayer tunneling for

their existence.[21,22] Further evidence of the rich variety of 2LQH states at $\nu_T=1$ comes from measuring the effects of an in-plane magnetic field, which induces a transition between two types of quantum Hall ground states.[12] These effects have been discussed in terms of an unusual broken-symmetry quantum Hall ground states that exhibit spontaneous interlayer (phase) coherence (SILC).[9,10]

At sufficiently small layer separation, a 2LQH system is an unusual quantum itinerant ferromagnet.[5,9,10] The SILC 2LQH quantum ferromagnet exhibits a rich variety of ground states, phase transitions, and charged and neutral excitations.[10,23] Murphy *et al.* investigated the effect of an in-plane magnetic field $B_\parallel$ on 2LQH systems, and found evidence of a phase transition between two competing QH ground states at a critical value $B_\parallel=B_c$.[12] These two ground states have been explained theoretically[9] by showing that application of a sufficiently strong parallel magnetic field $B_\parallel>B_c$ produces a soliton-lattice (SL) ground state in the incommensurate phase of the 2LQH system. Recent measurements of the interlayer tunneling conductivity in bilayer quantum-Hall samples have provided dramatic evidence for interlayer phase coherence.[24]

A. Effective Hamiltonian

Formally, it is simplest to obtain the ground-state characteristics of the SILC 2LQH state from the energy per unit area within a gradient approximation[9] in which the pseudospin $\mathbf{m}(\mathbf{r})$ is assumed to vary slowly on the scale of the magnetic length l. In doing so, it is convenient to specify the order parameter $\mathbf{m}(\mathbf{r})$ in terms of two quantities: $m_z(\mathbf{r})$, the local difference in layer occupancies, and $\theta(\mathbf{r})$, the projected angle of $\mathbf{m}$ in the xy plane measured with respect to the x axis. For constant $m_z=\nu_1-\nu_2$ and in-plane magnetic field $\mathbf{B}_\parallel$, the energy per unit area of the SILC 2LQH state has the form[9,10,23]

$$\mathcal{E}=\frac{1}{2\pi l^2}\left[-t\cos\tilde{\theta}+\frac{1}{2}\rho_s 2\pi l^2(\nabla\tilde{\theta}-\mathbf{Q})^2+\frac{U}{4}m_z^2-\frac{1}{2}V_g m_z\right], \tag{2.1}$$

where $\mathcal{E}$ has been expressed in terms of $\tilde{\theta}=\theta+\mathbf{Q}\cdot\mathbf{r}$, $\mathbf{Q}\equiv\hat{\mathbf{z}}\times\mathbf{B}_\parallel 2\pi d/\phi_0$, d is the interlayer spacing, and $\phi_0=h/e$ is the magnetic-flux quantum. Mean-field equations for $\tilde{\theta}$ and m_z are obtained by minimizing Eq. (2.1) with respect to those same quantities.

The first two terms of Eq. (2.1) constitute the Pokrovsky-Talapov (PT) model[7–9,25] with coefficients that, in the Hartree-Fock approximation (HFA), depend on m_z according to

$$t\equiv t_0\sqrt{1-m_z^2}e^{-Q^2l^2/4}=t_0\sqrt{4\nu_1\nu_2}e^{-Q^2l^2/4}$$

$$\rho_s\equiv\rho_0(1-m_z^2)=4\nu_1\nu_2\rho_0, \tag{2.2}$$

where t_0 is the tunneling-matrix element when $\nu_1=\nu_2$; it is equal to half the symmetric-antisymmetric gap Δ_{SAS}. In the presence of a parallel magnetic field,

$$t_0\rightarrow t_0\exp(-Q^2l^2/4), \tag{2.3}$$

which is a single-body effect.[26] The interlayer pseudospin stiffness when the layers are balanced is

$$\rho_0=\frac{e^2}{4\pi\epsilon l}\frac{1}{16\pi}\int_0^\infty dx x^2 e^{-x^2/2}e^{-xd/l} \tag{2.4}$$

in the HFA. The value of ρ_s will be reduced due to quantum fluctuations[27,28] and finite-thickness effects. By adjusting the front and back gate voltages of the sample, ν_1 and ν_2 may be varied (with $\nu_T\equiv\nu_1+\nu_2=1$), thereby allowing t and ρ_s to be adjusted.

The third term (quadratic in m_z) in the energy density [Eq. (2.1)] is a capacitive charging energy that favors equal layer densities.[9] The capacitive energy U is given in terms of the electrostatic Hartree energy ($\overline{D}_1$) and the intralayer ($\overline{E}_0$) and interlayer ($\overline{E}_1$) exchange energies by

$$U=\overline{D}_1-\overline{E}_0+\overline{E}_1,$$

$$\overline{D}_1=\frac{e^2}{4\pi\epsilon l}d/l,$$

$$\overline{E}_j=\frac{e^2}{4\pi\epsilon l}I_j\equiv\frac{e^2}{4\pi\epsilon l}\int_0^\infty dx e^{-x^2/2}e^{-xdj/l}, \tag{2.5}$$

where the exchange integrals I_j have been evaluated in the HFA. Most treatments of the SILC 2LQH state have been for equal layer densities ($m_z=0$), since there is a significant cost in capacitive charging energy to unbalance the layers.[9] However, an application of back and front gate voltages allows charge to be transferred from one layer to another, giving rise to a tunable nonzero value for m_z in the 2LQH ground state. The effects of charge-transfer imbalance were studied both theoretically and experimentally, and it was found that charge imbalance can actually *increase* the stability of the 2LQH state.[17,29,30]

We shall estimate the numerical values of our results for a hypothetical "typical" GaAs ($m^*\approx 0.07m_e$, $\epsilon_r\approx 13$) 2LQH sample,[16] with a total density $n_T=1.0\times10^{11}$ cm^{-2}, a layer (midwell to midwell) separation $d=20$ nm, and a tunneling energy $t_0=0.5$ meV ($\Delta_{SAS}=11.6$ K). Such a sample would have $l\approx 12.6$ nm, $d/l\approx 1.6$, $\hbar\omega_c\approx 6.9$ meV for $\nu_T=1$, and $e^2/4\pi\epsilon l\approx 8.8$ meV. In the HFA, $\rho_0\approx 0.03$ meV, $\overline{D}_1=14$ meV, and $U=7.4$ meV.

The effect of the gate voltages is described by the last (V_g) term in the energy density in terms of effective filling factors $\overline{\nu}_F$ and $\overline{\nu}_B$ for the front (F) and back (B) gates:

$$V_g=(\overline{\nu}_F-\overline{\nu}_B)\overline{D}_1. \tag{2.6}$$

The effective filling factors $\overline{\nu}_\alpha$ (where $\alpha=F,B$) are defined by the the electric fields E_α produced by the front and back

gates through Gauss' law $E_\alpha = e\bar{\nu}_\alpha/2\pi l^2\epsilon$, where ϵ (approximately $13\epsilon_0$ for GaAs) is the dielectric constant appropriate to the 2LQH sample.

B. Parallel magnetic field

When $Q \neq 0$, the pseudospin stiffness ρ_s competes with the rotating Zeeman pseudofield $t\cos\tilde{\theta}$ to determine the spatial orientations of the pseudospins. Minimizing $\mathcal{E}$ in Eq. (2.1) with respect to $\tilde{\theta}$ gives the two-dimensional sine-Gordon equation

$$\xi^2\nabla^2\tilde{\theta} = \sin\tilde{\theta}, \tag{2.7}$$

where the width of the soliton is proportional to the length,

$$\xi = \sqrt{2\pi\rho_s/t} = \xi_0(1-m_z^2)^{1/4}, \tag{2.8}$$

which for our hypothetical sample gives $\xi_0 \approx 17$ nm. The soliton width ξ sets the scale for spatial variations of the pseudospin $\mathbf{m}(\mathbf{r})$; thus the condition for the validity of the gradient approximation is that ξ be significantly larger than the magnetic length l.

For sufficiently small Q, Eq. (2.1) is minimized by $\tilde{\theta}(\mathbf{r}) = 0$. This is the commensurate (C) phase, and in this phase the pseudospins align themselves with the rotating Zeeman pseudofield, so that $\theta = -\mathbf{Q}\cdot\mathbf{r}$. However, above a critical value of $B_\parallel$ corresponding to $Q_c = 4/(\pi\xi) = (4/\pi l)\sqrt{t/2\pi\rho_s}$, it becomes energetically favorable to produce dislocation lines (solitons). The soliton widths are of order ξ. Solitons proliferate rapidly for $Q > Q_c$ (incommensurate phase) because they repel each other only very (exponentially) weakly (at zero temperature). The resulting array of solitons breaks the translational symmetry of the 2LQH ground state by forming a SL. For large $Q \gg Q_c$, the rapidly varying tunneling phase factor causes the pseudospins to behave (nearly) as if $t = 0$. In the HFA, the critical value of the in-plane field varies with the layer filling factors like $Q_c \propto (1-m_z^2)^{-1/4}$; thus tuning the layer filling factors (m_z) via gate voltages allows the location (Q_c) of the CI transtion to be fine tuned.

The density of soliton lines in the incommensurate phase is proportional to the soliton wave vector $Q_s = 2\pi/L_s$, where L_s is the spacing between solitons in the SL. The soliton density (proportional to Q_s) is calculated as a function of the in-plane field (proportional to Q) via two equations involving an intermediate parameter η. The parameter η is defined by[7,16]

$$Q_s/Q_c = (\pi/2)^2/[\eta K(\eta)], \tag{2.9}$$

approaches 1 near the CI transition ($Q_s \to 0$), and goes to 0 deep in the incommensurate phase ($Q_s \to \infty$). Here $K(\eta)$ is the complete elliptic integral of the first kind.[31]

When the layers are balanced ($\nu_1 = \nu_2$), minimizing the total energy with respect to Q_s gives[7,16]

$$Q/Q_c = E(\eta)/\eta, \tag{2.10}$$

where $E(\eta)$ is the complete elliptic integral of the second kind.[32] Equations (2.10) and (2.9) together determine the soliton density (or Q_s) as a function of the in-plane magnetic field (or Q). Q_s/Q_c is plotted as a function of Q/Q_c in Fig. 1, for the balanced case[16] ($m_z = 0$, solid curve) and for the rippled state ($m_z = 0.5$, dashed curve). Note the abrupt rise in soliton density for $Q > Q_c$. The compressional stiffness K_1 of the SL[16] is proportional to the slope of the Q_s versus Q curves in Fig. 1 (see Ref. 16):

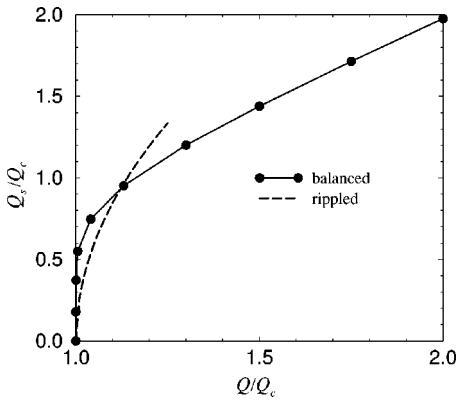

FIG. 1. Soliton density (times 2π) vs in-plane magnetic field for balanced layers ($m_z = 0$, solid curve) and for the rippled state ($m_{z0} = 0.5$, dashed curve). The soliton density rises abruptly in the incommensurate phase, $Q > Q_c$. There are no solitons in the commensurate phase, $Q < Q_c$.

$$\frac{\rho_s}{K_1} = \frac{\partial Q_s}{\partial Q}. \tag{2.11}$$

As expected, K_1 vanishes as $Q \to Q_c$.

C. Rippled layer imbalance

Minimizing Eq. (2.1) with respect to variations in m_z gives

$$m_z = \frac{V_g}{U + [2t\cos\tilde{\theta} - 4\pi l^2\rho_s(\nabla\tilde{\theta} - \mathbf{Q})^2]/(1-m_z^2)}. \tag{2.12}$$

This equation determines (in the Hartree-Fock gradient approximation) the filling factor of each layer for the $\nu_T = 1$ SILC state. For sufficiently small in-plane magnetic fields ($Q < Q_c$), $\tilde{\theta} = 0$ (the commensurate state), and the assumption that m_z is constant is self-consistent, provided that $t \ll U$.[23] However, when $Q \geq Q_c$, the quantum Hall ground state breaks translational invariance: $\tilde{\theta}$ is *not* spatially uniform and the soliton-lattice state is obtained.[9] When $Q \geq Q_c$ and $\bar{\nu}_1 \neq \bar{\nu}_2$, Eq. (2.12) shows that m_z also breaks translation invariance, and one obtains "rippled" layer densities. Thus uniform m_z is not consistent with the broken translation symmetry of $\tilde{\theta} = 0$ in the incommensurate phase, when $\bar{\nu}_1 \neq \bar{\nu}_2$. The resulting behavior of $m_z(\mathbf{r})$ is illustrated in Fig. 2.

It is important to note that Eq. (2.12) is valid even in the incommensurate state of spatially varying $\tilde{\theta}$, but only to first order in t/U. Since t/U is small in the bilayer samples studied so far, this assumption is not too restrictive. From now on, we shall work only to lowest non-trivial order in t/U, and

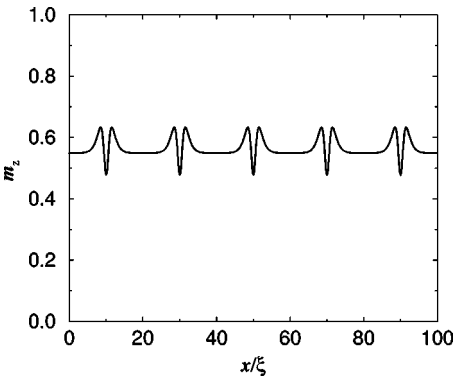

FIG. 2. Rippled layer imbalance $m_z(x)$ vs position for a soliton lattice with spacing $L_s/\xi=20$ between soliton lines. We have used the parameters for the ''typical'' sample described in the text, and taken $m_{z0}=0.5$. For these parameters, $\bar{m}_{z1}=0.048$.

expand m_z as described in the Appendix. Thus we shall not include the effect of the rippling of m_z on the soliton width ξ, since this would produce only small corrections (i.e., of higher order in t/U) to the results presented here. The soliton width ξ in Eq. (2.8) is therefore computed using $m_z \approx m_{z0}$, where m_{z0} is the layer imbalance in the absence of interlayer tunneling, as defined in the Appendix. The value of m_{z0} depends on the gate voltage V_g, but not on the ''rippling'' effect (which is of higher order in t/U).

Because $m_z=\nu_1-\nu_2$ is associated with differences in layer electron densities, the rippling has the effect of associating an electric-dipole density with each soliton. When the solitons are separated ($L_s>\xi$), the dipole-moment per unit length is (see the Appendix)

$$\frac{\delta p}{\delta y}=-\frac{ed\xi_0}{2\pi l_0^2}\frac{2t_0}{U}\frac{m_{z0}}{(1-m_{z0}^2)^{1/4}}(4Q/Q_c-3), \quad (2.13)$$

which has a value of about $-0.10e$ when $m_{z0}=0.5$ and $Q=Q_c$. Because the solitons have associated dipole moments, the dominant interactions between solitons when the solitons are separated will be their dipole-dipole repulsion. In the limit that the solitons are well separated ($L_s \gg \xi,d$), the interaction per unit length between two solitons separated by a distance x is

$$\frac{\mathcal{V}}{L}=\frac{(\delta p/\delta y)^2}{2\pi\epsilon x^2}, \quad (2.14)$$

so that the solitons repel each other with a force that falls off with distance as an inverse power (for $\nu_1\neq\nu_2$), rather than exponentially (for $\nu_1=\nu_2$). Summing all the the dipole-dipole soliton interactions gives, in the thermodynamic limit,

$$\frac{\mathcal{V}}{L_xL_y}=\frac{\pi}{12}\frac{(\delta p/\delta y)^2}{\epsilon L_s^3}=\frac{1}{96\pi^2}\frac{(\delta p/\delta y)^2}{\epsilon}Q_s^3, \quad (2.15)$$

which is proportional to $(t/U)^2$ and is therefore small in magnitude. However, near the CI transition, the solitons are well separated and dipole interactions dominate the repulsions between the solitons, which has a strong effect on the compressional stiffness K_1 of the SL. The relation between the wave vector Q and the parameter η is obtained by minimizing the total energy per unit area with respect to Q_s at fixed Q (Ref. 16); when the layers are balanced, Eq. (2.10) results, and Eqs. (2.9) and (2.10) may be combined to obtain Q_s as a function of Q. When the layers are imbalanced, Eq. (2.10) acquires an additional term due to the dipole interactions between solitons,

$$Q/Q_c=E(\eta)/\eta+\frac{1}{\rho_sQ_c}\frac{\partial}{\partial Q_s}\frac{\mathcal{V}}{L_xL_y}=E(\eta)/\eta+C(Q_s/Q_c)^2, \quad (2.16)$$

where $C\sim 0.14$ for the hypothetical ''typical'' sample with $m_{z0}=0.5$ and $Q=Q_c$. Near the CI transition Eq. (2.16) gives

$$Q_s/Q_c\approx\sqrt{(Q/Q_c-1)/C},$$

$$K_1/\rho_s\approx 2\sqrt{C(Q/Q_c-1)}. \quad (2.17)$$

The corresponding formula for the balanced ($\nu_1=\nu_2$) case are quite different: $Q_s\sim -1/\ln(Q-Q_c)$ and $K_1\sim(Q-Q_c)$, up to logarithmic corrections. Nonetheless, K_1 (and, by definition, Q_s) vanishes at the CI transition which has important consequences for the capacitance near the CI transition.

D. Topological charge

We also note that when the layers are imbalanced, the soliton lines acquire a charge density when they are tilted or sheared. In the lowest Landau level, the pseudospin textures with topological charge possess an electric charge. The electric-charge density $\delta\rho(\mathbf{r})$ is just the topological-charge density (i.e., the Pontryagian index density[10]) times $-e\nu_T$,

$$\delta\rho=\frac{e\nu_T}{8\pi}\epsilon_{ij}\mathbf{m}\cdot(\partial_i\mathbf{m}\times\partial_j\mathbf{m}), \quad (2.18)$$

where ϵ_{ij} is the totally antisymmetric tensor of rank 2, and we sum over i and j over the values 1 and 2 (x and y). The total filling factor is defined as $\nu_T=\nu_1+\nu_2$. Expression (2.18) in terms of m_z and θ using

$$m_x=\sqrt{1-m_z^2}\cos\theta, \quad m_y=\sqrt{1-m_z^2}\sin\theta \quad (2.19)$$

gives

$$\delta\rho(\mathbf{r})=\frac{e\nu_T}{4\pi}(\partial_x\theta\partial_y m_z-\partial_x m_z\partial_y\theta)$$

$$=\frac{e\nu_T}{4\pi}[(\partial_x\tilde{\theta}-Q)\partial_y m_z-\partial_x m_z\partial_y\tilde{\theta}], \quad (2.20)$$

where we have taken $\mathbf{Q}$ to be along the $\hat{\mathbf{x}}$ direction. If we rotate the soliton lines by taking

$$\tilde{\theta}_0(x)\rightarrow\tilde{\theta}_0(\alpha x+\beta y), \quad (2.21)$$

and also transform the rippled layer imbalance according to

$$\delta m_{z1}(x)\rightarrow\delta m_{z1}(\alpha x+\beta y), \quad (2.22)$$

then the associated charge density is

$$\delta\rho = -\frac{e\nu_T}{4\pi} Q \partial_y \delta m_{z1}(\alpha x + \beta y), \tag{2.23}$$

which associates a spatially varying charge density proportional to $\beta t/U$ to the tilted soliton lines. The integrated charge of the soliton lines remains zero, so the shear stiffness[16] may not be greatly affected.

E. Anisotropic transport

Application of a sufficiently strong in-plane magnetic field produces soliton lines that are parallel to the in-plane magnetic field. When the layers are imbalanced, these soliton lines possess dipole-charge densities. The resulting electric fields associated with the dipole-charge densities will make the conductivity anisotropic in the incommensurate phase. Transport parallel to the soliton lines (along the direction of the in-plane magnetic field, say $-\hat{\mathbf{y}}$) is expected to be easier than in the direction perpendicular (along $\hat{\mathbf{x}}$) to the soliton lines: i.e., when the layers are imbalanced, we expect

$$\rho_{xx} \approx \rho_{yy}, \quad Q < Q_c,$$
$$\rho_{xx} > \rho_{yy}, \quad Q > Q_c. \tag{2.24}$$

Thus a disparity between the longitudinal resistivities parallel and perpendicular to the in-plane magnetic field indicates the presence of an incommensurate soliton-lattice phase in the imbalanced system.

We note that anisotropic transport in the quantum Hall regime has been found in a very different context, in very high-mobility single-layer samples at high half-integer filling factors.[32,33] In this case, the anisotropic transport is taken to indicate the presence of a spontaneously striped anisotropic charge density of the quantum Hall ground state.[34] Here, the stripes are not spontaneous (for $t \ll U$), but are produced and oriented by the in-plane magnetic field. Nonetheless, the stripes (dipolar soliton lines) found here should also produce anisotropic transport.

III. INTERLAYER CAPACITANCE

Capacitance measurements offer the possibility of directly probing the ground-state properties of two-dimensional electron systems, such as the thermodynamic compressibility. Although the differential gate capacitance, which measures how the charge on a gate changes with respect to changes in the gate voltage, is slightly affected by the compressibility of the electron gas in the occupied layer that is nearest the gate, it is almost entirely dominated by the large gate-to-layer distance of the device. A far more sensitive measurement of the electronic compressibility is provided by the Eisenstein ratio R_E, which is an interlayer capacitance,[35–37]

$$R_E = \delta E_{12}/\delta E_{\text{gate}}, \tag{3.1}$$

where E_{12} is the electric field that exists between the layers, and E_{gate} is the electric field between the gate and the nearest layer. Classically, conduction electrons in the layers should completely screen the electric fields produced by the gates, so that $E_{12}=0$ and $R_E=0$. Indeed, this result is approached when the layers are sufficently far apart (beyond several hundred Å). But, due to their finite density of states, the effectively two-dimensional electron layers cannot completely screen the gate electric fields, so E_{12} is nonzero when the gates are unbalanced.

The Eisenstein ratio has been measured experimentally in two-dimensional electron gas (2DEG) systems, and used to determine the negative compressibility of the low-density 2DEG;[35] it has also been calculated theoretically at zero magnetic field[35,37] and in 2LQH systems.[36] The calculation of the Eisenstein ratio is discussed in some detail in Refs. 35–37; here we shall briefly outline only the key steps.

It is covenient to separate the total energy per unit area of the 2LQH system into an electrostatic part (i.e., the integrated electrostatic energy density $\epsilon E_{12}^2 d/2$ between the layers) and a many-body part $\langle \varepsilon \rangle$, which would be the energy per area for a system with neutralizing charge backgrounds in each layer.[36] The chemical potential relative to the bottom of quantum well i is given by[35]

$$\mu_i = \partial\langle\varepsilon\rangle/\partial n_i, \tag{3.2}$$

where $n_i = \nu_i/2\pi l^2$ is the areal number density in layer i. R_E can be expressed in terms of the interlayer separation d and the effective electronic lengths s_{ij}, defined as

$$s_{ij} = \frac{\epsilon}{e^2}\frac{\partial \mu_i}{\partial n_j} = \frac{l}{2}\frac{\partial^2}{\partial \nu_j \partial \nu_i}\left(\frac{2\pi l^2 \langle \varepsilon \rangle}{e^2/4\pi\epsilon l}\right), \tag{3.3}$$

from which it follows that $s_{ji}=s_{ij}$. In the absence of interlayer interactions (the case considered in Ref. 35), $s_{12}=s_{21}=0$ and the length s_{ii} is inversely proportional to the electronic compressibility κ_i in layer i (Ref. 36):

$$s_{ii} = \frac{\epsilon}{e^2 n_i^2 \kappa_i}. \tag{3.4}$$

If the front-gate and back-gate voltages are varied simultaneously so that the total layer density is kept fixed ($\nu_1 + \nu_2 = 1$), then

$$R_E \equiv \delta E_{12}/\delta E_{\text{gate}} = \frac{s_1 + s_2}{d + s_1 + s_2}, \tag{3.5}$$

where

$$s_1 \equiv s_{11} - s_{12}, \quad s_2 \equiv s_{22} - s_{21}. \tag{3.6}$$

If only one of the gate voltages is kept fixed, then the numerator of Eq. (3.5) is equal to either s_1 or s_2, instead of their sum.[37] At high densities, s_i (and thus R_E) are positive, but at suffiently low densities, they become negative, resulting in the negative values of R_E that have been measured experimentally.[35]

The Eisenstein ratio has been calculated for a $\nu_T=1$ 2LQH state,[36] although without a parallel magnetic field. It was found that, although the lengths s_i were negative, the criterion for stability against abrupt interlayer charge transfer,[37]

$$d + s_1 + s_2 > 0, \tag{3.7}$$

is still satisfied. It follows from Eqs. (3.5) and (3.7) that when R_E diverges, it signals an interlayer charge-transfer instability.

In the next two subsections, we calculate the contribution R_{E1} of the PT Hamiltonian to the Eisenstein ratio. R_{E1} contains the dependence of R_E on the tunneling t, pseudospin stiffness ρ_s, parallel magnetic field Q, and layer imbalance m_{z0}. It is convenient to separate R_{E1} into two parts: one that is formally divergent at $Q=Q_c$ when the layers are unbalanced ($m_z \neq 0$), and one that does not diverge, but which nevertheless exhibits a nontrivial dependence on Q and m_{z0}.

A. Divergent contribution

We shall first consider only the contributions to the electronic lengths s_i that become negative and divergent at the CI transition. We therefore focus on how changes in the layer imbalance m_z allow one to cross through the CI transition, due to the m_z dependence of the critical parallel magnetic field (or of Q_c), as discussed in Sec. II B and in Ref. 16. We therefore consider only the PT part of the the energy per area in Eq. (2.1), and then only that part of the PT energy that depends on m_z through Q/Q_c. (There are other terms that contribute to s_i, but they do not give rise to a divergence at the CI transition, at least for $t/U \ll 1$, which is the usual situation in most samples.) Because we are focusing on the effects of passing throught the CI transition, rather than the effects of changing the total filling factor, we restrict our attention to the case of fixed total filling factor ν_T. With these restrictions, the effect of taking a derivative of a function of Q/Q_c with respect to the layer filling factor ν_i produces the equivalence

$$\frac{\partial}{\partial \nu_i} \rightarrow -\frac{\partial m_z}{\partial \nu_i}\frac{\partial Q_C}{\partial m_z}\frac{Q}{Q_c}\frac{\partial}{\partial Q} = \frac{(-1)^i}{2}\frac{m_z}{1-m_z^2} Q \frac{\partial}{\partial Q}. \tag{3.8}$$

Combining Eqs. (3.3) and (3.8) with the magnetization calculations of Ref. 16 gives

$$\frac{s_1+s_2}{l} \sim -\pi\left(\frac{m_z}{1-m_z^2}\right)^2 (Ql)^2 \frac{\rho_s}{e^2/4\pi\epsilon l}\frac{\partial Q_s}{\partial Q}, \tag{3.9}$$

where we have kept only the contribution that diverges at the CI transition. The divergence occurs because nonzero m_z allows small changes in the layer filling factors to tune the system through the CI transition. The divergent part of the electronic lengths s_i are thus proportional to the in-plane differential magnetic susceptibility that was calculated in Ref. 16, and which diverges at the CI transition.

Unfortunately, the divergence in the electronic lengths s_i at the CI transition is weak, proportional to $1/\sqrt{Q-Q_c}$, with a small prefactor. For the hypothetical sample considered in this paper and $m_{z0}=0.5$, Eqs. (2.17) and (3.9) give

$$\frac{s_1+s_2}{l} \sim -\frac{0.005}{\sqrt{Q/Q_c-1}}, \tag{3.10}$$

which requires $(Q/Q_c-1)\sim 10^{-5}$ to give a divergent value of the Eisenstein ratio (i.e., $d+s_1+s_2=0$), at least for a tunneling-matrix element $t_0=0.5$ meV. The required nearness to the CI transition (i.e., the smallness of Q/Q_c-1) is inversely proportional to t_0, so making t_0 smaller might be of some help. However, it may be that in practice, sample disorder smears out the CI transition well before the divergence in R_E can be approached.

B. Nondivergent contributions

We saw in Sec. III A that, although there is a contribution to the interlayer capacitance (the Eisenstein ratio R_E) which is formally divergent at the CI transition, it may be difficult in practice to tune close enough to the transition to observe the divergence. It may be that the nondivergent contribution of the PT contribution to R_E is more easily detected. We calculate this contribution below for small $2t_0/U$.

For simplicity, we focus on the case of fixed total filling factor. Then it follows from the definition of R_E in Eq. (3.1), from Gauss' law, from the definition of V_g in Eq. (2.6), and from Eq. (2.12), that we may express R_E as

$$R_E = 1-\frac{\overline{D_1}}{U}\frac{\partial\langle m_z\rangle}{\partial m_{z0}} \approx R_{E0}+R_{E1},$$

$$R_{E0} = 1-\overline{D_1}/U,$$

$$R_{E1} = -\frac{\overline{D_1}}{U}\frac{\partial\langle m_{z1}\rangle}{\partial m_{z0}} = \frac{2t_0}{U}\left[\frac{\langle\cos\tilde{\theta}_0\rangle}{(1-m_{z0}^2)^{-3/2}} - \xi_0^2\langle(\nabla\tilde{\theta}_0-\mathbf{Q})^2\rangle\right]. \tag{3.11}$$

The largest contribution to the Eisenstein ratio is R_{E0}, and it was this quantity that was calculated in Ref. 36. For the hypothetical sample parameters in the text, $R_{E0}=-0.9$, independent of m_{z0} and Q. $R_E=R_{E0}$ when the interlayer-tunneling amplitude t_0 is very small, or when the parallel field is large (Q substantially larger than Q_c).

R_{E1} contains all the dependence of R_E on the in-plane magnetic field and layer imbalance. If t/U is made as large as possible, then by measuring the Q and m_{z0} dependence of R_E, it may be possible to measure R_{E1}. In the commensurate phase ($Q<Q_c$), $\tilde{\theta}_0=0$, so

$$R_{E1} = -\frac{\overline{D_1}}{U}\frac{2t_0/U}{\sqrt{1-m_{z0}^2}}\left[\frac{1}{(1-m_{z0}^2)}-\left(\frac{4}{\pi}\frac{Q}{Q_c}\right)^2\right]. \tag{3.12}$$

In the absence of an in-plane magnetic field ($Q=0$),

$$R_{E1}(Q=0) = -\frac{\overline{D_1}}{U}\frac{2t_0/U}{\sqrt{1-m_{z0}^{3/2}}} \approx -0.39, \tag{3.13}$$

for the hypothetical sample parameters described in the text, with $m_{z0}=0.5$, so that in this case R_{E1} is almost half the size of R_{E0}. As Q increases, R_{E1} decreases in magnitude and,

provided that $m_{z0} < \sqrt{1-(\pi/4)^2} \approx 0.62$, passes through zero and becomes positive near the CI transition.

At the CI transition, this nondivergent part of R_{E1} is

$$R_{E1}(Q=Q_c) = \frac{\bar{D}_1}{U} \frac{2t_0/U}{\sqrt{1-m_{z0}^2}} \left[\left(\frac{4}{\pi} \right)^2 - \frac{1}{(1-m_{z0}^2)} \right], \tag{3.14}$$

which for the sample parameters described in the text has a value of $R_{E1}(Q=Q_c)=0.16$ for $m_{z0}=0$ and $R_{E1}(Q=Q_c)=0.08$ for $m_{z0}=0.5$. In the incommensurate phase, R_{E1} drops rapidly to zero due to rapid spatial variations in $\tilde{\theta}_0(x)$.[16] By measuring how the in-plane magnetic field and layer imbalance affect the interlayer capacitance R_E, it may be possible to estimate the pseudospin stiffness ρ_s in the commensurate phase, and also to detect the incommensurate phase, as signaled by a rapid decrease in the sensitivity of R_E to Q and M_{z0}.

IV. CONCLUSIONS

It has been shown that the incommensurate phase of a bilayer quantum Hall state has a ''rippled'' dipole charge density whenever the layers are unbalanced. The rippling arises because the layer imbalance m_z and the interlayer phase θ are coupled through the m_z dependence of the effective tunneling energy t and pseudospin stiffness ρ_s in the Pokrovsky-Talapov part of the total energy in Eq. (2.1). This coupling between the layer imbalance and interlayer phase produces the rippled state when the translational symmetry of the phase is broken in the incommensurate phase. The rippled layer imbalance was calculated within the Hartree-Fock-gradient approximation and is illustrated in Fig. 2. The details of the calculation are given in the Appendix. We focused on the limit where the interlayer-tunneling energy is smaller than the charging energy of the bilayer ($t \ll U$), which is the case for all bilayer samples which have been studied experimentally so far.

Because solitons have an associated dipole-moment per unit length (which we estimated in the Appendix) in the rippled state, well-separated soliton lines experience a power-law (inverse cube) repulsive-force per unit length, rather than the much weaker exponentially-decaying repulsion between solitons found in the balanced case. This has a strong effect on how the density of solitons depends on the in-plane magnetic field near the CI transition, as illustrated in Fig. 1.

The fact that solitons have an electric dipole moment in the rippled state makes it likely that they produce anisotropic transport. Transport parallel to the soliton lines ($\pm\hat{\mathbf{y}}$) is likely to be easier than transport perpendicular to the soliton lines ($\pm\hat{\mathbf{x}}$). We expect the ratio ρ_{xx}/ρ_{yy} to increase when the rippled state is entered. This could provide an experimental signature for the incommensurate state.

We calculated the interlayer capacitance, specifically the Eisenstein ratio R_E, which is a sensitive measure of the electronic compressibility and of interlayer electronic correlations. When the layers are unbalanced, there is a contribution to R_E which diverges at the CI transition. However, observing this contribution is likely to be problematic because it requires that the CI transition be very sharp (unsmeared by disorder). We also calculated a contribution to R_E which does not diverge at the CI transition, but which nevertheless offers a good possibility of experimental detection. We calculated the in-plane magnetic-field dependence of R_E, along with its dependence on layer imbalance, especially in the commensurate ($Q<Q_c$) phase, up to the CI transition ($Q=Q_c$), and discussed its behavior (rapid decline) in the incommensurate ($Q>Q_c$) phase. By measuring R_E, the pseudospin stiffness could be estimated and the incommensurate phase detected.

The existence of ''rippled'' layer densities in the incommensurate phase of unbalanced 2LQH systems is expected to be valid beyond the HFGA, although the size of the density variations will be reduced by quantum fluctuations.[27,28] As long as the layer densities are ''rippled,'' they will make an anomalous contribution to the capacitance. Although fluctuation effects change the sizes of ρ_s and t,[27,28] the basic physics of producing ''rippled'' layer densities still holds beyond the HFA. In particular, ρ_s and t will still change with the layer imbalance m_z, and this dependence on m_z will produce a coupling between m_z and the pseudospin angle θ, leading to nonuniform m_z in the incommensurate phase when $\nu_1 \neq \nu_2$.

Several remarks about the observability of the capacitive effects found here are in order, especially the effects of including finite temperature and disorder. In practice, both finite temperature and disorder limit the minimum effective value of (Q/Q_c-1) that can be obtained. These are important topics which deserve further study; only some preliminary considerations are discussed here.

Ignoring the effects of disorder for the moment, it is important to note that the soliton lattice exists only at sufficiently low temperatures. The soliton lattice supports a finite-temperature Kosterlitz-Thouless (KT) transition due to dislocation-mediated melting of the lattice of soliton lines.[8,38] The KT temperature for melting the soliton lattice is roughly $k_B T_{KT} \sim (\pi/2)\sqrt{K_1 K_2}$, where K_1 is the longitudinal stiffness and K_2 is the transverse stiffness of the soliton lattice.[13] Because $K_1 \to 0$ as $Q \to Q_c$, the KT temperature drops as the CI transition is approached. This sets a limit to how close one can get to the CI transition, which may be estimated in the case of finite layer imbalance by using $K_1 = 2\sqrt{C(Q/Q_c-1)}$ [see Eq. (2.17)] and $K_2 = \rho_s$.[16] From these considerations, the requirement that $T < T_{KT}$ gives

$$(Q/Q_c-1) > \frac{1}{4}\left(\frac{2}{\pi} \frac{k_B T}{\rho_s} \right)^4 \approx 2.4 \left(\frac{T}{1\ \mathrm{K}} \right)^4 \tag{4.1}$$

for the sample parameters used in the text. For $T=100$ mK, this yields $(Q/Q_c-1) > 2.4\times 10^{-4}$.

The smearing of the CI transition due to disorder is more problematic. Even in capacitance experiments designed to measure the (in)compressibility of the fractional quantum hall (FQH) state (which would, in the absence of disorder, lead to a divergent R_E at odd-denominator filling factors), only finite changes in R_E are found at the FQH filling factors, due to the effects of disorder.[35] It is to be expected that

disorder may eliminate any abrupt features in the interlayer capacitance R_E in this case also. Strictly speaking, the long-range order of the SL is destroyed by any finite amount of disorder;[39] presumably the SL has only a finite correlation length $\zeta_d < \infty$ due to disorder. Roughly speaking, the maximum spacing between solitons (L_s) will be limited to $L_s < \zeta_d$, so that

$$(Q/Q_c - 1) > C\left(\frac{\pi^2}{2}\frac{\xi}{\zeta_d}\right)^2. \tag{4.2}$$

In practice, such disorder could arise from small variations in the local tunneling ampitudes t or the spin stiffness ρ_s due to minute variations in the interlayer barrier thickness and/or the layer separation. More theoretical work needs to be done to determine the limits imposed by disorder, but the issue of the observability of the CI transition in capacitance measurements must be settled experimentally.

ACKNOWLEDGMENTS

The author gratefully acknowledges helpful discussions with A. H. MacDonald and S. M. Girvin. It is a pleasure to thank A. R. Hamilton for answering several questions regarding experimental measurements on double-layer systems. Thanks are also due to R. J. Reimann and G. R. Newby for useful discussions. This work was supported by an award from Research Corporation and by NSF Grant No. DMR-997232. The author is thankful for the support provided by the ITP Scholars Program at U. C. Santa Barbara, where part of this work was carried out; thus this research was also supported in part by the National Science Foundation under Grant No. PHY99-07949. In addition, the work described is supported by the NSF-Idaho EPSCoR Program and by the National Science Foundation under Award No. EPS-0132626.

APPENDIX: DIPOLE MOMENT

In this Appendix, we estimate the dipole-moment per unit length associated with solitons in the incommensurate phase of an imbalanced 2LQH system. Expanding Eq. (2.1) in powers of (t/U) gives

$$m_z(\mathbf{r}) \approx m_{z0} + m_{z1}(\mathbf{r}), \tag{A1}$$

where

$$m_{z0} = V_g/U \tag{A2}$$

is the $t=0$ result for the layer imbalance, and

$$m_{z1}(\mathbf{r}) = \frac{2t}{U}\frac{m_{z0}}{(1-m_{z0}^2)}[\xi^2(\nabla\tilde{\theta}_0 - \mathbf{Q})^2 - \cos\tilde{\theta}_0], \tag{A3}$$

to first order in t/U. Here $\tilde{\theta}_0(\mathbf{r})$ is the soliton-line solution to the PT model for the values of t and ρ_s corresponding to setting $m_z = m_{z0}$ in Eq. (2.2).

For a single soliton, the lowest-order solution for $\tilde{\theta}$ is[16]

$$\tilde{\theta}_0(x) = 4\arctan\exp(x/\xi), \tag{A4}$$

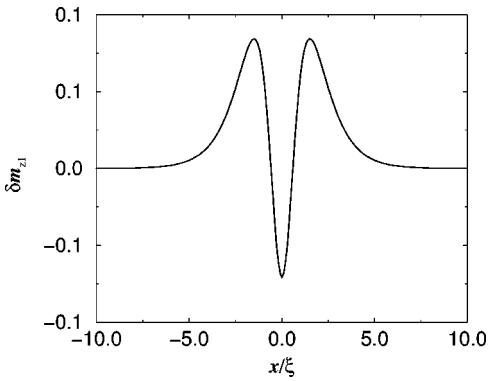

FIG. 3. Spatial dependence of the layer imbalance $\delta m_{z1}(x)$ associated with a single soliton, vs position for the hypothetical ''typical'' sample parameters described in the text.

where we have taken $\mathbf{Q}$ to lie along the $\hat{\mathbf{x}}$ direction. This gives

$$1 - \cos\tilde{\theta}_0(x) = \frac{2}{\cosh^2(x/\xi)},$$

$$\xi\partial_x\tilde{\theta}_0(x) = \frac{2}{\cosh(x/\xi)}. \tag{A5}$$

It is convenient to express $m_{z1}(\mathbf{r})$ as

$$m_{z1}(\mathbf{r}) = \bar{m}_{z1} + \delta m_{z1}(x), \tag{A6}$$

where

$$\bar{m}_{z1} = \frac{2t}{U}\frac{m_{z0}}{(1-m_{z0}^2)}(Q^2\xi^2 - 1) \tag{A7}$$

is the value of m_{z1} in the commensurate ($\tilde{\theta}_0 = 0$) phase. For the hypothetical sample described in the text, $\bar{m}_{z1} \approx 0.048$ for $m_{z0} = 0.5$ and $Q \approx Q_c$. We associate the spatially-dependent part of m_z (see Fig. 3) with the soliton line:

$$\delta m_{z1}(x) = \frac{2t}{U}\frac{m_{z0}}{(1-m_{z0}^2)}\left[\frac{4Q\xi}{\cosh(x/\xi)} - \frac{6}{\cosh^2(x/\xi)}\right]. \tag{A8}$$

The areal number density of layer j is given by $n_j = \nu_j/(2\pi l^2)$. Therefore, the dipole-moment per unit area is

$$\frac{p}{L_x L_y} = -\frac{ed}{2\pi l^2}m_z, \tag{A9}$$

and we associate an dipole-moment per unit length

$$\frac{\delta p}{\delta y} = -\frac{ed}{2\pi l^2}\int_{-\infty}^{\infty} \delta m_{z1}(x)dx$$

$$= -\frac{ed\xi}{2\pi l^2}\frac{8t}{U}\frac{m_{z0}}{(1-m_{z0}^2)}(\pi Q\xi - 3)$$

$$= -\frac{ed\xi_0}{2\pi l_0^2}\frac{2t_0}{U}\frac{m_{z0}}{(1-m_{z0}^2)^{1/4}}(4Q/Q_c - 3). \quad \text{(A10)}$$

For the ''typical'' sample described in Sec. II A at layer imbalance $m_{z0}=1/2$ and $Q=Q_c$,

$$\delta p/\delta y \approx -0.10e, \quad \text{(A11)}$$

where $-e$ is the electric charge of an electron.

When the soliton lines do not overlap (Q sufficiently near Q_c), then $\tilde{\theta}_0(x)$ is very nearly a periodic superposition of single-soliton solutions, spaced apart by L_s:

$$\tilde{\theta}_0(\mathbf{r}) \approx 4\sum_j \arctan\exp[(x-jL_s)/\xi]. \quad \text{(A12)}$$

The dipolar interaction-energy per unit length between two parallel soliton lines separated by a distance x is

$$\frac{\mathcal{V}_2(x)}{L_y} = \frac{(\delta p/\delta y)^2}{2\pi\epsilon x^2}. \quad \text{(A13)}$$

Thus the total dipole-interaction energy per unit area is

$$\frac{\mathcal{V}}{L_xL_y} = \frac{N_s}{L_xL_y}\sum_{j=1}^{\infty}\mathcal{V}_2(jL_s) = \frac{\pi}{12}\frac{(\delta p/\delta y)^2}{\epsilon L_s^3}$$

$$= \frac{1}{96\pi^2}\frac{(\delta p/\delta y)^2}{\epsilon}Q_s^3, \quad \text{(A14)}$$

where we have used the fact that the number of solitons is $N_s = L_z/L_s$.

The relation between the wave vector Q and the parameter η is obtained by minimizing the total energy per unit area with respect to Q_s at fixed Q;[16] when the layers are balanced, Eq. (2.10) results, and Eqs. (2.9) and (2.10) may be combined to obtain Q_s as a function of Q. When the layers are imbalanced, Eq. (2.10) acquires an additional term due to the dipole interactions between solitons,

$$Q/Q_c = E(\eta)/\eta + \frac{1}{\rho_s Q_c}\frac{\partial}{\partial Q_s}\frac{\mathcal{V}}{L_xL_y} = E(\eta)/\eta + C(Q_s/Q_c)^2, \quad \text{(A15)}$$

where

$$C = \frac{1}{8\pi}\left(\frac{\delta p/\delta y}{e}\right)^2\frac{e^2/4\pi\epsilon l}{\rho_s}Q_c l, \quad \text{(A16)}$$

and $C\sim 0.14$ for the hypothetical ''typical'' sample with $m_{z0}=0.5$ and $Q=Q_c$. Because the interaction between separated solitons is an inverse-power law (when unbalanced) rather than exponetially decaying function (when balanced), Q_s and K_1 are proportional to $\sqrt{Q-Q_c}$ near the CI transition.

[1] D.C. Tsui, H.L. Störmer, and A.C. Gossard, Phys. Rev. Lett. **48**, 1559 (1982).

[2] *The Quantum Hall Effect*, edited by R. E. Prange and S. M. Girvin (Springer-Verlag, New York, 1990), and references therein.

[3] R.B. Laughlin, Phys. Rev. Lett. **50**, 1395 (1983).

[4] S.L. Sondhi, A. Karlhede, S.A. Kivelson, and E.H. Rezayi, Phys. Rev. B **47**, 16 419 (1993).

[5] See S. M. Girvin and A. H. MacDonald, in *Perspectives in Quantum Hall Effects*, edited by S. Das Sarma and A. Pinczuk (Wiley, New York, 1997), and references therein.

[6] G. Grüner, *Density Waves in Solids* (Addison-Wesley, New York, 1995), and references therein.

[7] P. Bak, Rep. Prog. Phys. **45**, 587 (1982).

[8] Marcel den Nijs, in *Phase Transitions in Critical Phenomena*, edited by C. Domb and J. L. Lebowitz (Academic Press, New York, 1988), Vol. 12, pp. 219–333.

[9] K. Yang, K. Moon, L. Zheng, A.H. MacDonald, S.M. Girvin, D. Yoshioka, and S.C. Zhang, Phys. Rev. Lett. **72**, 732 (1994).

[10] K. Moon, H. Mori, K. Yang, S.M. Girvin, A.H. MacDonald, L. Zheng, D. Yoshioka, and S.C. Zhang, Phys. Rev. B **51**, 5138 (1995).

[11] S.M. Girvin and A.H. MacDonald, Phys. Rev. Lett. **58**, 1252 (1987).

[12] S.Q. Murphy, J.P. Eisenstein, G.S. Boebinger, L.N. Pfeiffer, and K.W. West, Phys. Rev. Lett. **72**, 728 (1994).

[13] N. Read, Phys. Rev. B **52**, 1926 (1995).

[14] K. Moon and K. Mullen, Phys. Rev. B **57**, 1378 (1998).

[15] C.B. Hanna, A.H. MacDonald, and S.M. Girvin, Physica B **249-251**, 824 (1998).

[16] C.B. Hanna, A.H. MacDonald, and S.M. Girvin, Phys. Rev. B **63**, 125305 (2001).

[17] C.B. Hanna, Bull. Am. Phys. Soc. **42**, 553 (1997).

[18] Y.N. Joglekar and A.H. MacDonald, Phys. Rev. B **65**, 235319 (2002).

[19] Leo Radzihovsky, Phys. Rev. Lett. **87**, 236802 (2001).

[20] M. Abolfath, L. Radzihovsky, and A.H. MacDonald, Phys. Rev. B **65**, 233306 (2002).

[21] J.P. Eisenstein, G.S. Boebinger, L.N. Pfeiffer, K.W. West, and S. He, Phys. Rev. Lett. **68**, 1383 (1992); Y.W. Suen, L.W. Engel, M.B. Santos, M. Shayegan, and D.C. Tsui, *ibid.* **68**, 1379 (1992).

[22] A.H. MacDonald, Surf. Sci. **229**, 1 (1990).

[23] K. Yang, K. Moon, L. Belkhir, H. Mori, S.M. Girvin, A.H. MacDonald, L. Zheng, and D. Yoshioka, Phys. Rev. B **54**, 11 644 (1996).

[24] I.B. Spielman, J.P. Eisenstein, L.N. Pfeiffer, and K.W. West, Phys. Rev. Lett. **84**, 5808 (2000); **87**, 036803 (2001).

[25] V.L. Pokrovsky and A.L. Talapov, Phys. Rev. Lett. **42**, 65 (1970); Zh. Éksp. Teor. Fiz. **78**, 269 (1980) [Sov. Phys. JETP **51**, 134 (1980)].

[26] J. Hu and A.H. MacDonald, Phys. Rev. B **46**, 12 554 (1992).
[27] K. Moon, Phys. Rev. Lett. **78**, 3741 (1997).
[28] Yogesh N. Joglekar and Allan H. MacDonald, Phys. Rev. B **64**, 155315 (2001).
[29] A.R. Hamilton, M.Y. Simmons, F.M. Bolton, N.K. Patel, I.S. Millard, J.T. Nicholls, D.A. Ritchie, and M. Pepper, Phys. Rev. B **54**, R5259 (1996).
[30] A. Sawada, Z.F. Ezawa, H. Ohno, Y. Horikoshi, A. Urayama, Y. Ohno, S. Kishimoto, F. Matsukura, and N. Kumada, Phys. Rev. B **59**, 14 888 (1999); A. Sawada, Z.F. Ezawa, H. Ohno, Y. Horikoshi, O. Sugie, S. Kishimoto, F. Matsukura, Y. Ohno, and M. Yasumoto, Solid State Commun. **103**, 447 (1997).
[31] I. S. Gradshteyn and I. M. Ryzhik, *Table of Integrals, Series, and Products* (Academic Press, New York, 1980), Sec. 8.1.
[32] M.P. Lilly, K.B. Cooper, J.P. Eisenstein, L.N. Pfeiffer, and K.W. West, Phys. Rev. Lett. **82**, 394 (1999); **83**, 824 (1999).
[33] R.R. Du, D.C. Tsui, H.L. Störmer, L.N. Pfeiffer, K.W. Baldwin, and K.W. West, Solid State Commun. **109**, 389 (1999).
[34] A.A. Koulakov, M.M. Fogler, and B.I. Shklovskii, Phys. Rev. Lett. **76**, 499 (1996); M.M. Fogler, A.A. Koulakov, and B.I. Shklovskii, Phys. Rev. B **54**, 1853 (1996).
[35] J.P. Eisenstein, L.N. Pfeiffer, and K.W. West, Phys. Rev. B **50**, 1760 (1994); Phys. Rev. Lett. **68**, 674 (1992).
[36] T. Jungwirth and A.H. MacDonald, Phys. Rev. B **53**, 9943 (1996).
[37] C.B. Hanna, Dylan Haas, and J.C. Díaz-Vélez, Phys. Rev. B **61**, 13 882 (2000).
[38] Thermal fluctuations will renormalize the SL stiffness and lead to other interesting effects; for recent work, see: E. Papa and A. Tsvelik, cond-mat/0201343 (unpublished); S. Park, K. Moon, C. Ahn, J. Yeo, C. Rim, and B.H. Lee, cond-mat/0203498 (unpublished).
[39] M.P.A. Fisher (private communication).